Structural and magnetic dimers in the spin-gapped system $CuTe_2O_5$

J. Deisenhofer,[1] R. M. Eremina,[2,3] A. Pimenov,[2] T. Gavrilova,[3] H. Berger,[4] M. Johnsson,[5] P. Lemmens,[6] H.-A. Krug von Nidda,[2] A. Loidl,[2] K.-S. Lee,[7,8] and M.-H. Whangbo[7]

[1]*Département de Physique de la Matière Condensée, Université de Genève, CH-1211 Genève 4, Switzerland*
[2]*EP V, Center for Electronic Correlations and Magnetism, Augsburg University, D-86135 Augsburg, Germany*
[3]*E. K. Zavoisky Physical-Technical Institute, 420029 Kazan, Russia*
[4]*Institute de Physique de la Matière Complexe, EPFL, CH-1015 Lausanne, Switzerland*
[5]*Department of Inorganic Chemistry, Stockholm Univ., S-10691 Stockholm, Sweden*
[6]*Institute for Physics of Condensed Matter, Technical University of Braunschweig, D-38106 Braunschweig, Germany*
[7]*Department of Chemistry, North Carolina State University, Raleigh, NC 27695-8204, USA*
[8]*Department of Chemistry, The Catholic University of Korea, Bucheon, Gyeonggi-Do, South Korea 422-743*

(Dated: February 6, 2008)

We investigated the magnetic properties of the system $CuTe_2O_5$ by susceptibility and electron spin resonance measurements. The anisotropy of the effective g-factors and the ESR linewidth indicates that the anticipated structural dimer does not correspond to the singlet-forming magnetic dimer. Moreover, the spin susceptibility of $CuTe_2O_5$ can only be described by taking into account interdimer interactions of the same order of magnitude than the intradimer coupling. Analyzing the exchange couplings in the system we identify the strongest magnetic coupling between two Cu ions to be mediated by super-super exchange interaction via a bridging Te ligand, while the superexchange coupling between the Cu ions of the structural dimer only results in the second strongest coupling.

PACS numbers: 76.30.-v, 71.70.Ej, 75.30.Et, 75.30.Vn

I. INTRODUCTION

Transition-metal-compounds based on Cu^{2+} ions with a $3d^9$ configuration exhibit an enormously rich variety of magnetic structures depending on the effective magnetic dimensionality of the system.[1] Introducing lone-pair cations like Se^{4+} or Te^{4+} into the magnetic system was suggested as a fruitful path to tailor the magnetic dimensionality and to create new magnetic structures.[2,3] For example, it was proposed that $Cu_2Te_2O_5X_2$ (X=Cl, Br), which consists of tetrahedral clusters of Cu^{2+} linked by bridging Te-O units, is an example of quasi-zero-dimensional systems in which the extreme limits of magnetic insulation via Te^{4+} ions are reached.[4] The transition from a spin-gapped paramagnetic state to an antiferromagnetically ordered state at $T_N = 18.2$ K (X=Cl) and $T_N = 11.4$ K (X=Br) was attributed to the proximity of a quantum phase transition.[5] The magnetization, specific heat and Raman scattering data of $Cu_2Te_2O_5Br_2$ were also interpreted by considering weakly coupled Cu_4 tetrahedra within a mean field approximation.[5] Recently, this understanding in terms of weakly-interacting tetramers has been questioned by a spin dimer analysis, which showed that the spin exchange interactions between adjacent Cu^{2+} sites are much weaker within each Cu_4 tetrahedron than between adjacent Cu_4 tetrahedra.[6] Additionally, electronic band structure calculations for $Cu_2Te_2O_5X_2$ (X=Cl, Br) have confirmed the presence of strong interactions between adjacent Cu_4 tetrahedra.[7]

The compound investigated in this study is the related system $CuTe_2O_5$ which exhibits a monoclinic structure with space group P21/c and lattice parameters $a = 6.871$Å, $b = 9.322$Å, $c = 7.602$Å, $\beta = 109.08°$.[8] The lattice consists of pairs of strongly distorted and edge-sharing CuO_6 octahedra with a Cu-Cu distance of 3.18 Å. These structural dimer units (see Fig. 1) are separated by Te-O bridging ligands and a Cu-Cu distance of 5.28 Å. The magnetic susceptibility of $CuTe_2O_5$ shows a maximum at $T_{max} = 56.6$ K and a strong decrease for lower temperatures, which can be roughly modeled by isolated magnetic dimers. The high-temperature susceptibility corresponds to a Curie-Weiss law with a Curie-Weiss temperature of $\Theta = -41$ K.[1] In this study we investigate the spin susceptibility of $CuTe_2O_5$ by electron spin res-

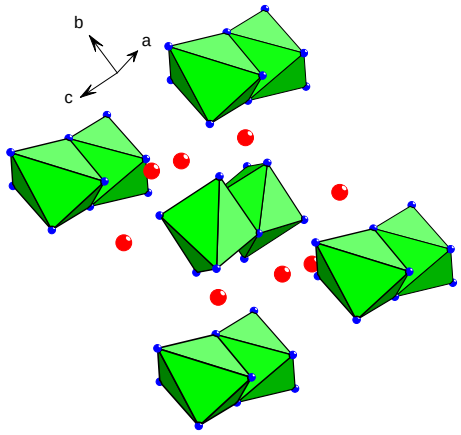

FIG. 1: (Color online) Crystal structure of $CuTe_2O_5$ (space group $P21/c$). The Cu_2O_{10} dimer units (edge-sharing octahedra) are separated by Te ions (large spheres).

onance (ESR) and dc-susceptibility measurements. By analyzing the spin susceptibility and the exchange paths within and between the structural dimers based on extended Hückel tight binding (EHTB) electronic structure calculations, we determine the magnetic structure of the system and find that it differs significantly from the one intuitively imposed by the lattice structure.

II. SAMPLE PREPARATION AND EXPERIMENTAL DETAILS

Large single crystals of $CuTe_2O_5$ in form of platelets with a maximum size of 8x8x0.5 mm^3 were grown by the usual halogen vapor transport technique, using HBr as transport agents. The charge and growth-zone temperatures were 580 °C and 450 °C respectively. The stoichiometry of obtained single crystals was quantitatively probed by electron-probe microanalysis. The compound crystallizes as large blue-green plates and was characterized also by X-ray diffraction. Powder samples have been prepared in sealed quartz ampules using stoichiometric molar ratios of CuO and TeO_2.

Susceptibility measurements were performed on single crystals and polycrystalline samples using a SQUID magnetometer (Quantum Design). ESR measurements were performed in a Bruker ELEXSYS E500 CW-spectrometer at X-band (9.47 GHz) and Q-band (34 GHz) frequencies equipped with continuous He-gas-flow cryostats (Oxford Instruments) in the temperature range $4.2 \leq T \leq 300$ K. ESR detects the power P absorbed by the sample from the transverse magnetic microwave field as a function of the static magnetic field H. The signal-to-noise ratio of the spectra is improved by recording the derivative dP/dH using lock-in technique with field modulation. The $CuTe_2O_5$ single crystal was glued on a suprasil-quartz rod, which allowed the rotation of the sample around defined crystallographic axes. High-field ESR was performed at a frequency of 185 GHz using a quasi optical technique with backward-wave oscillators as coherent sources for submillimeter wavelength radiation.[9,10] The spectrometer is equipped with a superconducting split-coil magnet with a maximum field of 8T.

III. EXPERIMENTAL RESULTS

As shown in Fig. 2 the observed ESR absorption is well described by a single exchange narrowed Lorentzian line with resonance field $H_{\rm res}$ and half-width at half maximum linewidth ΔH except for temperatures below 20 K, where the ESR intensity $I_{\rm ESR}$ strongly decreases due to the singlet formation of the dimers and the residual signal remains from defects giving rise to a complicated splitting of the spectrum like e.g. in $CuGeO_3$ below the spin-Peierls transition.[11]

Therefore, we will concentrate in the following on the

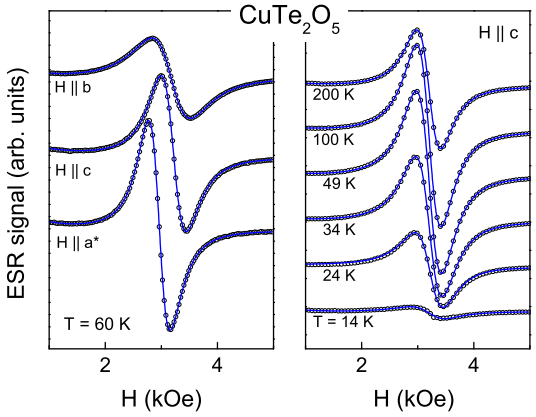

FIG. 2: (Color online) ESR spectra in $CuTe_2O_5$ at $T = 60$ K for the external magnetic field parallel to the main crystallographic directions (left column) and at different temperatures for $\mathbf{H} \parallel c$ (right column). The solid lines represent fits with a Lorentzian line shape.

temperature regime above 20 K. In the investigated temperature regime the g values are practically temperature independent with $g_{a^*} = 2.27(2)$, $g_b = 2.11(3)$, and $g_c = 2.10(2)$, where a^* denotes the direction perpendicular to the b-c plane. Such g values slightly enhanced with respect to the spin-only value of $g = 2$ are typical for the $3d^9$ electronic configuration of Cu^{2+} in distorted oxygen octahedra, where the orbital momentum is nearly quenched by the crystal field.[12]

Figure 3 shows the full angular dependence of the g tensor in three perpendicular crystallographic planes at room temperature. It is nearly constant in the b-c plane and increases monotonously from b to a^*. But within the a^*-c plane the principal axes of the tensor turn out to be tilted by about 30° with respect to the a^* axis. Here the g tensor exhibits its maximum at $g_{\rm max} = 2.30(2)$ and minimum at $g_{\rm min} = 2.06(2)$. The a^*-c plane contains the real crystallographic a axis at the monoclinic angle $\beta = 109.08°$, but this does not coincide with one of the principal axes of the g tensor.

The corresponding angular dependence of the linewidth at 300 K is depicted in Fig. 4. The data approximately coincide for X-band and Q-band frequency. The largest variation of the linewidth appears in the a^*-b plane where it monotonously increases from 300 Oe up to 500 Oe on rotating the magnetic field from the a^* direction into the b direction. On further rotating the field into the c direction the linewidth is monotonously reduced to 350 Oe. Again, in the a^*-c plane the extrema of the linewidth do not coincide with a^* and c direction, but are tilted by about 10° with respect to these directions. The temperature dependence of the linewidth is not very pronounced down to about 100 K. As shown in Fig. 5(b), the linewidth increases with decreasing temperature up to about 750 Oe at 25 K for $H \parallel b$ followed by a decrease to lower temperatures, whereas the increase is much weaker for the two other orientations.

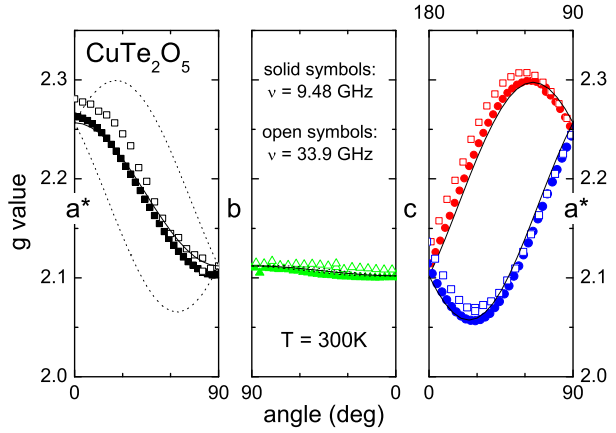

FIG. 3: (Color online) Angular dependence of the g factor for three perpendicular crystallographic planes at room temperature for X-band and Q-band frequencies. The solid lines represent a fit of the g tensor assuming two inequivalent Cu sites, the contributions of which are indicated by dotted lines. (Right frame: bottom abscissa: upper data set; top abscissa: lower data set.)

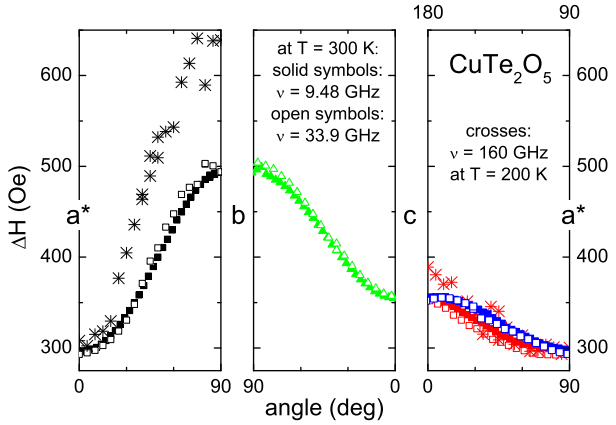

FIG. 4: (Color online) Angular dependence of the linewidth for three perpendicular crystallographic planes at 300 K for X-band and Q-band frequencies, and for the $a^* - b$- and the $a^* - c$-plane (spheres) measured at 200 K and 160 GHz. (Right frame: bottom abscissa: lower data and crosses; top abscissa: upper data)

The temperature dependence of the ESR intensity obtained by double integration of the ESR signal perfectly coincides with the temperature behavior of the dc-susceptibility (see Fig. 5(a)). Thus, the static susceptibility indeed is dominated by the pure spin susceptibility represented by the ESR intensity - diamagnetic and van Vleck contributions are negligible. Before we analyze the spin susceptibility in detail in the next section, we want to discuss the difficulties occurring in the evaluation of g tensor and linewidth, if the system is assumed to consist of nearly isolated magnetic dimers as suggested from the crystal structure.

We try to describe the angular dependence of the g tensor using purely structural considerations. Each Cu^{2+} ion is surrounded by an oxygen octahedron which is elongated along the O2-O5′ axis (see inset of Fig. 5(a)), with distances Cu-O5′=2.303 Å and Cu-O2=2.779 Å. But the Cu-O distances within the plane, built up by the other four oxygen ions, differ only within 0.04 Å, with the smallest distances for Cu-O5 of 1.948 Å, and Cu-O3 of 1.969 Å.[8] Note that because of the asymmetric elongation of the octahedra, the ground-state orbital will have a small admixture of the $d_{3z^2-r^2}$-orbital. As an approximation, however, we assume that also in the present geometry the hole of the $3d^9$ state occupies the $d_{x^2-y^2}$ orbital located in this plane. This gives rise to a g tensor diagonal in a local cartesian coordinate system with two axes approximately given by Cu-O1 (x) and Cu-O5 (y) and the z axis (with the largest g value) perpendicular to the plane. The oxygen octahedra of two Cu^{2+}-ions within one dimer are just rotated by 180° against each other and, therefore, should have the same g-tensor. Hence, to describe the anisotropy of the g-value, one has to sum up the local g-tensors of the two dimers with different orientation in the unit cell. The best fit yielding $g_{xx} = 2.029$, $g_{yy} = 2.105$, and $g_{zz} = 2.329$ is shown in Fig. 3 as solid lines together with the single contributions (dotted lines) of the two dimers of different orientation. The strongest effect of the two inequivalent places is visible in the a^*-b plane, whereas it is only weak in the b-c plane and vanishes completely in the a^*-c plane. In the dimer model this should influence the line broadening in the a^*-b plane via the anisotropic Zeeman effect as will be illustrated in the following.

In general, the ESR linewidth in the case of sufficiently strong exchange interaction can be analyzed in terms of the high-temperature Kubo-Tomita approach:[13]

$$\Delta H_\infty = \frac{1}{g\mu_B} \cdot \frac{M_2}{J}, \qquad (1)$$

where ΔH_∞ corresponds to the high-temperature value of the ESR linewidth, μ_B denotes the Bohr magneton, J is the isotropic exchange constant, and M_2 yields the second moment

$$M_2 = h^2\langle(\nu - \nu_0)^2\rangle = \frac{\langle[\mathcal{H}_{\rm int}, S^+]\,[S^-, \mathcal{H}_{\rm int}]\rangle}{\langle S^+ S^-\rangle} \qquad (2)$$

of the ESR absorption line. It has been shown for several antiferromagnetic spin $S = 1/2$ chain compounds (e.g. $LiCuVO_4$ and $CuGeO_3$) with a similarly large linewidth like $CuTe_2O_5$ that the anisotropic exchange interactions are the dominant contributions to the microscopic spin Hamiltonian $\mathcal{H}_{\rm int}$.[14,15,16,17] Therefore, we believe that the ESR linewidth in $CuTe_2O_5$ is dominated by the anisotropic exchange, as well. Besides this broadening mechanism, the anisotropic Zeeman interaction mentioned above is expected to be of importance in the a^*-b plane, where the difference of the g values of both inequivalent Cu sites yields a contribution to the second

moment which is proportional to the square of the applied magnetic field . Details are described by Pilawa for the case of $CuGeO_3$, where a similar situation occurs due to two inequivalent Cu chains.[18] Assuming that the inter-dimer isotropic exchange interaction, which is responsible for the narrowing of the anisotropic Zeeman contribution, is much weaker than the intra-dimer isotropic exchange interaction, this contribution to the line broadening should be largest for an angle of 45° in the a^*-b plane, where the difference in g values of both sites is largest, but should vanish for 0° and 90°, where the g values are equal. Moreover, this contribution should gain importance with increasing frequency due to its quadratic field dependence.

However, such an anisotropic Zeeman contribution to the linewidth cannot be detected at X-band and Q-band frequencies (c.f. Fig. 4), where the data approximately coincide within the experimental uncertainty. Therefore, we performed additional high-field ESR measurements at 160 GHz and at 185 GHz. Having investigated the orientation dependence of the linewidth at 200 K and 160 GHz (see Fig.4), we found that a strong increase of the linewidth is observed in the a^*-b plane, but changes within the a^*-c plane are very small as compared to the X/Q-band data and remain within the experimental uncertainty, although one may want to infer a slight tendency to an additional line broadening along the c-axis, which would be in agreement with the expectation for an anisotropic Zeeman contribution. Consequently, we measured the temperature dependence of the linewidth with the magnetic field oriented along the a^*- and the b axis (shown together with the X-Band data in Fig. 5(b)) at a higher frequency of 185 GHz and a correspondingly higher magnetic field. Note that the increase is maximal for the magnetic field applied along the b direction in contrast to the expectation resulting from the analysis of the g tensor. This discrepancy indicates that the assumed dimer model, which is based on the structural Cu_2O_{10} units, does not properly describe the magnetic properties of $CuTe_2O_5$. Maybe also the g tensors of the inequivalent Cu sites deviate from the orientation suggested by the structural data and a possible admixture of the $d_{3z^2-r^2}$-orbital will give important contributions and has to be taken into account in order to obtain a consistent description oft he ESR data. Therefore, a detailed analysis of the microscopic exchange paths (as will be presented in Section IV.B) has to be performed before one can try to understand the ESR behavior in this compound.

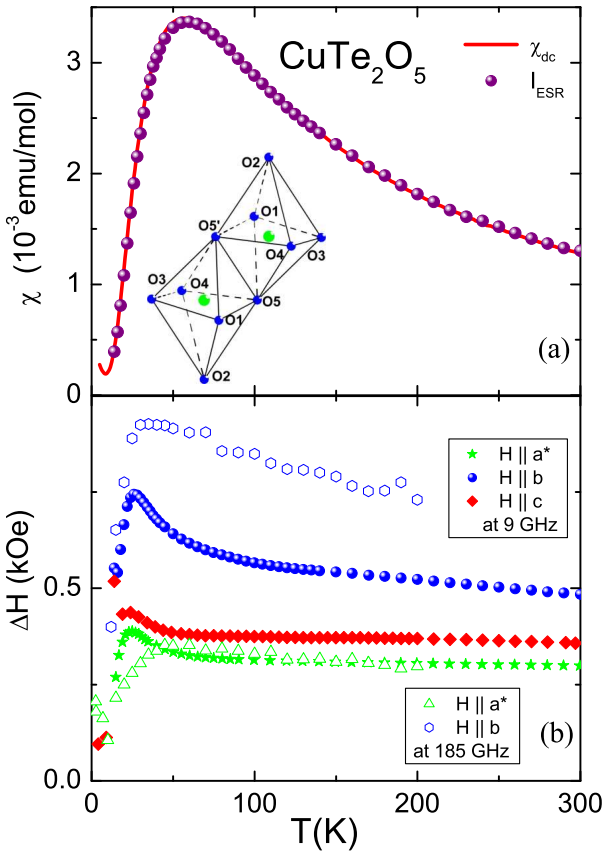

FIG. 5: (Color online) Temperature dependences of (a) the ESR intensity and the dc susceptibility (Inset: Cu_2O_10 structural dimer), (b) the ESR linewidth in $CuTe_2O_5$ with the external magnetic field applied along the crystallographic axes for 9 GHz and 185 GHz.

Finally, we briefly comment on the temperature dependence of the linewidth: Concerning the maximum of the linewidth at low temperatures, we plot the product of the linewidth data with the spin susceptibility multiplied by the temperature in Fig. 6. In the Kubo-Tomita approach the main temperature dependence of the ESR linewidth stems from the spin susceptibility:

$$\Delta H_{KT}(T) = \frac{1}{\chi(T)T} \cdot \Delta H_{\infty}, \qquad (3)$$

In this limit the product $\Delta H \cdot \chi \cdot T$ should become temperature independent for high temperatures and corresponds to the so called memory function. As recently reported by Chabre *et al.*[19] for the quasi one dimensional spin-gap system η-$Na_{1.286}V_2O_5$ the maxima in the temperature dependence of the linewidth (Fig. 5(b)) may just result from a monotonously increasing memory function in combination with the temperature dependence of the susceptibility. A similar temperature dependence of the memory function has been experimentally found and theoretically confirmed earlier by Pilawa *et al.* in the one-dimensional antiferromagnet tetraphenylverdazyl.[20] The memory function in our case behaves very similar to the above spin-chain compounds starting from zero at zero temperature with a monotonous increase and saturating at temperatures large compared to the exchange coupling J/k_B. Similar to the case of η-$Na_{1.286}V_2O_5$ the anomaly suggested by the maximum of the linewidth is not visible in the memory function any more and, therefore, we discard the possibility that the maximum arises due to changes in the magnetic structure of the system.

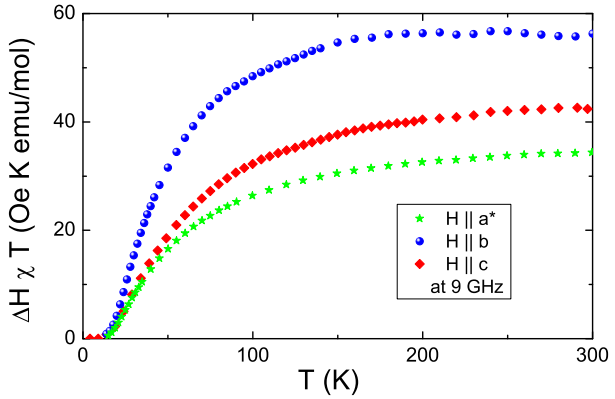

FIG. 6: (Color online) Temperature dependences of the memory function in $CuTe_2O_5$ with the external magnetic field applied along the crystallographic axes.

IV. DISCUSSION

A. Fit of the spin susceptibility

The usual ansatz to describe the spin susceptibility in dimer systems is

$$\chi = \chi_{VV} + \chi_C + \chi_{BB}, \tag{4}$$

where χ_{VV} denotes a possible Van-Vleck contribution, $\chi_C = C/T$ is a Curie contribution due to unbound spins and magnetic impurities, and χ_{BB} is the dimer susceptibility as derived by Bleaney and Bowers (BB)[21]:

$$\chi_{BB}(T) = \frac{Ng^2\mu_B^2}{k_BT}[3 + \exp(J/k_BT)]^{-1}, \tag{5}$$

where J denotes the intradimer exchange coupling, g is the effective g-factor, and μ_B is the Bohr magneton.

To account for possible couplings between the dimers we will take into account two different approaches. The first one is to substitute the BB-equation by the approach by Johnston *et al.* who calculated the susceptibility of a spin-1/2 antiferromagnetic chain with alternating exchange constants J_1 and J_2:[22]

$$\chi(\alpha, T) = \frac{Ng^2\mu_B^2}{k_BT}\chi^*(\alpha, T), \tag{6}$$

where $\alpha = J_2/J_1$ denotes the ratio of the antiferromagnetic coupling constants. The function $\chi^*(\alpha, T)$ has been obtained by various numerical methods to describe excellently the full range of susceptibilities from a pure Heisenberg dimer system with $\alpha = 0$ (corresponding to the Bleaney-Bowers equation) to a uniform Heisenberg spin chain with $\alpha = 1$. Although the system appears to be a three-dimensional network of structural dimers, it is well possible that there is one dominant interdimer exchange path which will effectively produce a lower magnetic dimensionality which can be modeled by an alternating spin chain behavior.

The second approach consists of a mean-field modification of the Bleaney-Bowers equation

$$\chi(T) = \frac{Ng^2\mu_B^2}{k_BT}[3 + \exp(J/k_BT) + J'/k_BT]^{-1}, \tag{7}$$

where J' is an effective coupling between Cu ions of two different magnetic dimers.[23]

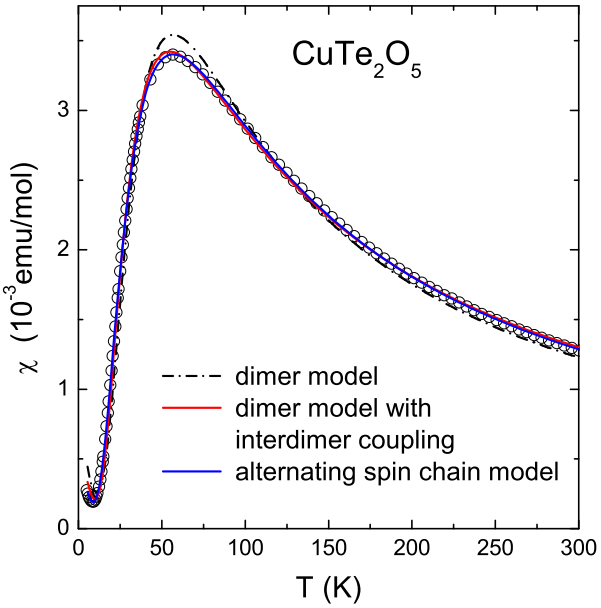

FIG. 7: (Color online) Temperature dependences of the spin susceptibility (circles) in $CuTe_2O_5$. The lines are best fits obtained by the models described in the text.

With the above models we tried to describe the spin susceptibility by obtaining the best fit results which are shown in Fig. 7. Note that the very good agreement between the dc-susceptibility and the ESR intensity allowed us to set $\chi_{VV} = 0$. Given the existence of structural dimers, we started to approximate the spin susceptibility by using $\alpha = 0$ corresponding to the simple dimer model by Bleaney and Bowers. The resulting best-fit curve is shown as the dash-dotted line in Fig. 7, yielding $J = 91.6$ K and $g = 1.92$ and $C = 2.44 \cdot 10^{-3}$ emu K/mol. Obviously, a pure dimer model fails to describe the susceptibility in the full temperature range and yields an effective g-factor considerably lower than the one obtained by ESR measurements.

Varying the ratio α freely, we were able to get an excellent fit (solid line in Fig.7) yielding the alternating exchange coupling constants $J_1 = 93.3$ K and $J_2 = 40.7$ K, i.e. a ratio $\alpha = J_2/J_1 = 0.436$, $C = 1.45 \cdot 10^{-3}$ emu K/mol, and an effective g-factor of $g = 1.99$, which is already in reasonable agreement with the values observed by ESR.

Using Eq. 7 we can get an equally good fit with parameters $J = 88.9$ K, $J' = 91.4$ K, $C = 1.84 \cdot 10^{-3}$ emu K/mol and a g-factor $g = 2.08$ which is in very good agreement

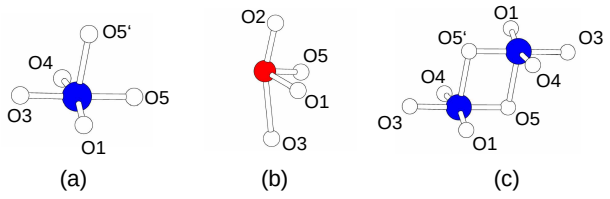

FIG. 8: (Color online) Building units of $CuTe_2O_5$: (a) CuO_5, (b) TeO_4 and (c) Cu_2O_8. The large, middle and small spheres show Cu, Te and O atoms, respectively.

with the experimentally obtained ones. Note that the effective inter-dimer exchange J' is slightly larger than the intra-dimer coupling yielding a ratio of $J'/J = 1.03$. It was shown by Sasago et al.[24] that such the mean-field approach does not allow to estimate the correct value of J' in the case $J'/J \simeq 1$. Therefore, the above values obtained by the mean-field equation have to be interpreted with caution, only allowing to state that the interdimer coupling is certainly not negligible in this case.

Although we cannot unambiguously determine the magnetic structure by fitting the susceptibility, we can conclude that both models, the alternating spin-chain and the modified BB approach, show that in $CuTe_2O_5$ the inter-dimer exchange coupling is of the same order of magnitude than the intra-dimer coupling. In addition to the difficulties in describing the ESR data by purely structural considerations, this finding corroborates that there exists at least one strong additional magnetic coupling between Cu ions which are separated by an intermediate Te ligand. To understand the appearance of such a considerable inter-dimer exchange, it is necessary to investigate in detail the possible exchange paths between adjacent Cu ions, which will be subject of the following section.

B. Analysis of the exchange paths

Starting out again from the crystal structure of $CuTe_2O_5$, we regard the system as being built up of CuO_5 square pyramids (Fig. 8a), which edge-share to form structural Cu_2O_8 dimers (Fig. 8c). These dimers corner-share with TeO_4 units (Fig. 8b) to form the three-dimensional lattice of $CuTe_2O_5$. The spin exchange interaction within the Cu_2O_8 dimer is a superexchange (SE) interaction since its two Cu^{2+} ions are linked by Cu-O-Cu bridges. Each Cu^{2+} ion of a CuO_5 square pyramid (i.e. a spin monomer) has one singly occupied $d_{x^2-y^2}$-block orbital (i.e. the magnetic orbital) that lies in the basal plane of the square pyramid. In a Cu_2O_8 dimer (Fig. 8c) the basal planes of the two CuO_5 square pyramids are parallel to each other, so that their magnetic orbitals cannot overlap well. Therefore, the interpretation of the structural dimer Cu_2O_8 as a magnetic dimer may not be justified. However, so far we have not taken into consideration the role of the TeO_4 units linking between CuO_5 square pyramids. Accounting for such TeO_4 units has been shown to change considerably the magnetic properties of $Cu_4Te_5O_{12}Cl_4$ with respect to $Cu_2Te_2O_5Br_2$.[25] In general, the spin exchange interactions of $CuTe_2O_5$ can take place through SE paths, Cu-O-Cu, or through super-superexchange (SSE) paths, Cu-O...O-Cu, in which the O...O contact is provided by TeO_4 units. It has been shown that SSE interactions can be strong in magnitude and can be even stronger than SE interactions, and hence must not be neglected.[26] Therefore, we evaluated the relative strengths of nine spin exchange interactions (shown in Fig. 9) in $CuTe_2O_5$ by performing a spin dimer analysis based on extended Hückel tight binding (EHTB) electronic structure calculations.[26,27,28]

TABLE I: Exponents ζ_i and valence shell ionization potentials H_{ii} of Slater-type orbitals ϕ_i used for extended Hückel tight-binding calculation. H_{ii} are the diagonal matrix elements $\langle\phi_i|H_{eff}|\phi_i\rangle$, where H_{eff} is the effective Hamiltonian. For the calculation of the off-diagonal matrix elements $H_{ij} = \langle\phi_i|H_{eff}|\phi_j\rangle$, the weighted formula as described in Ref. 31 was used. C and C' denote the contraction coefficients used in the double-zeta Slater-type orbital.

atom	ϕ_i	H_{ii}(eV)	ζ_i	C	ζ_i'	C'
Cu	4s	-11.4	2.151	1.0		
Cu	4p	-6.06	1.370	1.0		
Cu	3d	-14.0	7.025	0.4473	3.004	0.6978
Te	5s	-20.8	4.406	0.6568	1.652	0.4892
Te	5p	-13.2	3.832	0.5934	2.187	0.5402
O	2s	-32.3	2.688	0.7076	1.675	0.3745
O	2p	-14.8	3.694	0.3322	1.866	0.7448

The two magnetic orbitals of a spin dimer interact to give rise to an energy split Δe. In the spin dimer analysis based on EHTB calculations, the strength of an antiferromagnetic interaction between two spin sites is estimated by considering the antiferromagnetic spin exchange parameter $J_{AF} = -(\Delta e)^2/U_{eff}$,[26] where U_{eff} is the effective on-site repulsion that is essentially a constant for a given compound. Therefore, the trend in the J_{AF} values is determined by that in the corresponding values $(\Delta e)^2$.

TABLE II: Cu...Cu distances in Å, $(\Delta e)^2$ in $(\text{meV})^2$ for the spin exchange paths J_1-J_9 in $CuTe_2O_5$ shown in Fig. 9, and the relative strengths of the spin exchange interactions compared to the strongest interaction J_6.

exchange J_i	Cu...Cu distance	$(\Delta e)^2$	$(\Delta e)_i^2/(\Delta e)_6^2$
J_1	3.187	2250	0.59
J_2	5.282	200	0.05
J_3	5.322	520	0.14
J_4	5.585	410	0.11
J_5	5.831	40	0.01
J_6	6.602	3840	1.00
J_7	6.437	190	0.05
J_8	6.489	350	0.09
J_9	6.871	990	0.26

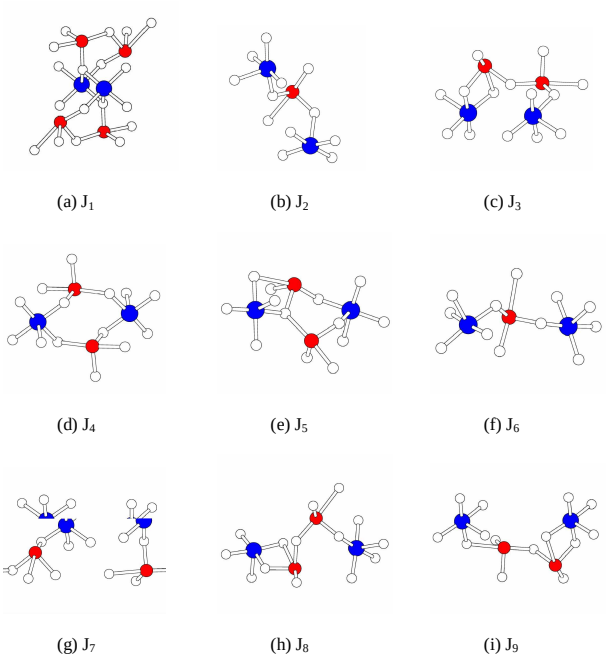

FIG. 9: (Color online) Spin dimers of $CuTe_2O_5$ associated with the spin exchange interactions J_1-J_9. The large, middle and small spheres show Cu, Te and O atoms, respectively.

The magnetic properties of a variety of magnetic solids are well described by the values obtained from EHTB calculations,[26] when both the d-orbitals of the transition metal and the s/p orbitals of its surrounding ligands are represented by double-zeta Slater type orbitals.[29] The atomic parameters used for the present EHTB calculations of the $(\Delta e)^2$ values are summarized in Table I. The exponents ζ and ζ' of the Slater type atomic orbitals Te 5s/5p listed in Table I are greater than those of the atomic orbital calculations[29] by the factor of 1.45, because such values are needed in reproducing the band gap of α-TeO_2 by EHTB calculations.[30]

The results of our examination of the spin dimers (i.e.the structural units containing two spin sites) in $CuTe_2O_5$ are listed in Table II. We identified the strongest interaction J_6 to be of antiferromagnetic SSE type mediated by O-Te-O bridges and the second strongest J_1 to be the antiferromagnetic SE interaction within the structural dimer Cu_2O_8, yielding a ratio $(\Delta e_1)^2/(\Delta e_6)^2 = J_1/J_6 = 0.59$. In terms of the description as an alternating spin chain this ratio is not too far away from the value $\alpha = 0.436$ resulting from the fit with Eq. 6. Therefore, the model of an alternating spin chain appears as the simplest possible model for $CuTe_2O_5$. The existence of further exchange paths such as J_3 and J_9 shows, however, that these spin chains would exhibit non-negligible couplings between each other. To unambiguously identify the magnetic structure in $CuTe_2O_5$ remains a challenging task for the future, including the experimental quest for further evidence to corroborate or discard the possibility of alternating spin chains as suggested by fitting the spin susceptibility.

The strength of a SSE interaction through the exchange path of the type Cu-O-L-O-Cu (e.g., L = Te, Se, P) depends sensitively on how the O-L-O linkage orients the two magnetic orbitals (i.e., the $d_{x^2-y^2}$ orbital orbitals) of the two Cu^{2+} sites and also on how the orbitals of the ligand atom L are oriented with respect to the two magnetic orbitals.[26] In $Cu_2Te_2O_5X_2$ (X=Cl,Br), two adjacent Cu_4 tetrahedra make Cu-O-Te-O-Te-O-Cu and Cu-X...X-Cu linkages, and it is the Cu-X...X-Cu paths that provide strong spin exchange interactions.[6] In $CuSe_2O_5$ the Cu^{2+} ions form chains of Cu-O-Se-O-Cu linkages leading to a uniform linear spin chain model.[32] In $CuTe_2O_5$ the spin exchange J_6 has a Cu-O-Te-O-Cu linkage that is quite symmetrical in shape, so the orbitals of the intervening TeO_2 unit provide a strong overlap with two $d_{x^2-y^2}$ orbitals of the two Cu^{2+} sites.

In general, our finding shows that the intuitive picture of the equivalence of structural and magnetic dimers can be misleading, as has been observed for a number of magnetic solids. For example, the strongest magnetic coupling in CaV_4O_9 appears between next-nearest-neighbor vanadium ions,[33,34] in contrast to the structurally suggestive picture of only weakly coupled plaquettes of V^{4+} ions. The singlet-forming Cu^{2+} ions in $CaCuGe_2O_6$ are given by the third-nearest-neighbor copper pairs that occur between chains of edge-sharing distorted CuO6 octahedra.[35,36] Both alternating chain and spin ladder models describe the magnetic susceptibility of $(VO)_2P_2O_7$ well,[37,38,39] but an alternating chain model was proven to be correct for $(VO)_2P_2O_7$ by neutron scattering experiments[40] on oriented single crystals and also by spin dimer analysis based on EHTB calculations.[41] All these examples demonstrate the importance of considering the overlap between magnetic orbitals in arriving at a correct spin lattice model.

V. CONCLUSIONS

Using electron spin resonance and susceptibility measurements we determined the spin susceptibility of the Cu-dimer system $CuTe_2O_5$. The obtained ESR data suggested that the structural dimers do not coincide with the magnetic dimers. The analysis of the spin susceptibility revealed a coupling of about 90 K within the magnetic dimer and a considerable inter-dimer coupling of the same order of magnitude. A detailed investigation of the magnetic exchange paths revealed the strongest magnetic coupling to be of super-superexchange type. Therefore, $CuTe_2O_5$ belongs to the interesting class of compounds like $CaCuGe_2O_6$ or $(VO)_2P_2O_7$, where the effective low energy Hamiltonian cannot simply be mapped on geometric aspects of the crystallographic structure. Eventually, such a discrepancy might be found in many low-dimensional compounds and it appears a challenging experimental and theoretical task to identify and classify

common parameters of such systems.

Acknowledgments

It is a pleasure to thank D. Zakharov for fruitful discussions. We acknowledge support by the BMBF via contract number VDI/EKM 13N6917 and partly by the DFG via SFB 484 (Augsburg), the Swiss NSF through the NCCR MaNEP, and by the RFBR (Grant No. 06-02-17401) and BRHE REC 007. The research was further supported by the Office of Basic Energy Sciences, Division of Materials Sciences, U. S. Department of Energy, under Grant DE-FG02-86ER45259. K.-S. L. thanks The Catholic University of Korea for the 2006-Research Fund.

[1] P. Lemmens, G. Güntherodt, C. Gros, Phys. Rep. **375**, 1 (2003).
[2] M. Johnsson, K.W. Tornroos, F. Mila, and P. Millet, Chem. Mater. **12**, 2853 (2000).
[3] M. Herak, H. Berger, M. Prester, M. Miljak, I. Zivkovic, O. Milat, D. Drobac, S. Popovic, and O. Zaharko, cond-mat/0507684 (2005).
[4] P. Lemmens, K.-Y. Choi, E.E. Kaul, C. Geibel, K. Becker, W. Brenig, R. Valenti, C. Gros, M. Johnsson, P. Millet, and F. Mila, Phys. Rev. Lett. **87**, 227201 (2001).
[5] C. Gros, P. Lemmens, M. Vojta, R. Valenti, K.-Y. Choi, H. Kageyama, Z. Hiroi, N.V. Mushnikov, T. Goto, M. Johnsson, and P. Millet, Phys. Rev. B **67**, 174405 (2003).
[6] M.-H. Whangbo, H.-J. Koo, D. Dai and D. Jung, Inorg. Chem. **42**, 3898 (2003).
[7] R. Valentí, T. Saha-Dasgupta, C. Gros, and H. Rosner, Phys. Rev. B **67**, 245110 (2003).
[8] K. Hanke, V. Kupcik, O. Lindqvist, Acta Cryst. B **29**, 963 (1973).
[9] G. V. Kozlov and A. A. Volkov, in *Millimeter and Submillimeter Wave Spectroscopy in Solids*, edited by G. Grüner, Springer, Berlin (1998).
[10] D. Ivannikov, M. Biberacher, H.-A. Krug von Nidda, A. Pimenov, A. Loidl, A. A. Mukhin, and A. M. Balbashov, Phys. Rev. B **65**, 214422 (2002).
[11] A. I. Smirnov, V. N. Glazkov, L. I. Leonyuk, A. G. Vetkin, and R. M. Eremina, Zh. Eksp. Teor. Fiz. **114**, 1876 (1998) [JETP **87**, 1019 (1998)].
[12] A. Abragam and B. Bleaney, *Electron Paramagnetic Resonance of Transition Ions*, Clarendon Press, Oxford (1970).
[13] R. Kubo and K. Tomita, J. Phys. Soc. Jpn. **9**, 888 (1954), P. W. Anderson and P. R. Weiss, Rev. Mod. Phys. **25**, 269 (1953).
[14] H.-A. Krug von Nidda, L. E. Svistov, M. V. Eremin, R. M. Eremina, A. Loidl, V. Kataev, A. Validov, A. Prokofiev, and W. Assmus, Phys. Rev. B **65**, 134445 (2002).
[15] R. M. Eremina, M. V. Eremin, V. N. Glazkov, H.-A. Krug von Nidda, A. Loidl, Phys. Rev. B **68**, 014417 (2003).
[16] M. V. Eremin, D. V. Zakharov, R. M. Eremina, J. Deisenhofer, H.-A. Krug von Nidda, G. Obermeier, S. Horn, and A. Loidl, Phys. Rev. Lett. **96**, 027209 (2006).
[17] D. V. Zakharov, J. Deisenhofer, H.-A. Krug von Nidda, P. Lunkenheimer, J. Hemberger, M. Hoinkis, M. Klemm, M. Sing, R. Claessen, M.V. Eremin, S. Horn, and A. Loidl, Phys. Rev. B **73**, 094452 (2006).
[18] B. Pilawa, J. Phys.: Condens. Matter **9**, 3779 (1997).
[19] F. Chabre, A. M. Ghorayeb, P. Millet, V. A. Pashchenko, A. Stepanov, Phys. Rev. B **72**, 012415 (2005).
[20] B. Pilawa and T. Pietrus, J. Magn. Magn. Mater. **150**, 165 (1995).
[21] B. Bleaney and K.D. Bowers, Proc. R. Soc. A **214**, 451 (1952).
[22] D.C. Johnston, R.K. Kremer, M. Troyer, X. Wang, A. Klumper, S.L. Bud'ko, A.F. Panchula, and P.C. Canfield, Phys. Rev. B **61**, 9558 (2000).
[23] T. Nakajima, H. Mitamura, and Y. Ueda, J. Phys. Soc. Jpn. **75**, 054706 (2006).
[24] Y. Sasago, M. Hase, K. Uchinokura, M. Tokunaga, and N. Miura, Phys. Rev. B 52, 3533 (1995).
[25] R. Takagi, M. Johnsson, V. Gnezdilov, R. K. Kremer, W. Brenig, and P. Lemmens, Phys. Rev. B **74**, 014413 (2006).
[26] For recent reviews, see: M.-H. Whangbo, H.-J. Koo, and D.J. Dai, Solid State Chem. **176**, 417 (2003); M.-H. Whangbo, D. Dai, and H.-J. Koo, Solid State Sci. **7**, 827 (2005).
[27] R. Hoffmann, J. Chem. Phys. **39**, 1397 (1963).
[28] Our calculations were carried out by employing the SAMOA (Structure and Molecular Orbital Analyzer) program package (Dai, D.; Ren, J.; Liang, W.; Whangbo, M.-H., http://chvamw.chem.ncsu.edu/, 2002).
[29] E. Clementi, C. Roetti, Atomic Data Nuclear Data Tables **14**, 177 (1974).
[30] E. Menéndez-Proupin, G. Gutierrez, E. Palmero, and J.L. Peña, Phys. Rev. B **70**, 035112 (2004).
[31] J. Ammeter, H.-B. Bürgi, J. Thibeault, and R. Hoffmann, J. Am. Chem. Soc. **100**, 3686 (1978).
[32] O. Kahn, M. Verdaguer, J.J. Girerd, J. Galy, and F. Maury, Solid State Commun. **34**, 971 (1980).
[33] W.E. Pickett, Phys. Rev. Lett. **79**, 1746 (1999).
[34] H.-J. Koo and M.-H. Whangbo, J. Solid State Chem. **153**, 263 (2000).
[35] R. Valenti, T. Saha-Dasgupta, and C. Gros, Phys. Rev. B **66**, 054426 (2002).
[36] H.-J. Koo, D. Dai and M.-H. Whangbo, Inorg. Chem. **44**, 4359 (2005).
[37] D.C. Johnston, J.W. Johnson, D.P. Goshorn, and A.J. Jacobson, Phys. Rev. B **35**, 219 (1987).
[38] T. Barnes and J. Riera, Phys. Rev. B **50**, 6817 (1994).
[39] D.C. Johnston, T. Saito, M. Azuma, M. Takano, T. Yamauchi, and Y.Ueda, Phys. Rev. B **64**, 134403 (2001)
[40] A. W. Garret, S. E. Nagler, D. A. Tennant, B. C. Sales and T. Barnes, Phys. Rev. Lett. **79**, 745 (1997).
[41] H.-J. Koo, M.-H. Whangbo, P. D. VerNooy, C. C. Torardi and W. J. Marshall, Inorg. Chem. **41**, 4664 (2002).